Liquid Crystals
Publication details, including instructions for authors and subscription information:
http://www.informaworld.com/smpp/title~content=t713926090

Effect of electron donor-acceptor interaction on the thermal stability of supramolecular side chain liquid crystalline polymers based on poly(3-carboxypropylmethylsiloxane)

Suat Hong Goh; Yee Hing Lai

Online publication date: 11 November 2010

To cite this Article Goh, Suat Hong and Lai, Yee Hing(2002) 'Effect of electron donor-acceptor interaction on the thermal stability of supramolecular side chain liquid crystalline polymers based on poly(3-carboxypropylmethylsiloxane)', Liquid Crystals, 29: 5, 675 — 685
To link to this Article: DOI: 10.1080/02678290210126040
URL: http://dx.doi.org/10.1080/02678290210126040

LIQUID CRYSTALS, 2002, VOL. 29, NO. 5, 675–685

Taylor & Francis
Taylor & Francis Group

Effect of electron donor–acceptor interaction on the thermal stability of supramolecular side chain liquid crystalline polymers based on poly(3-carboxypropylmethylsiloxane)

XU LI, SUAT HONG GOH* and YEE HING LAI

Department of Chemistry, National University of Singapore, 3 Science Drive 3, Singapore 117543

(*Received 14 August 2001; in final form 15 November 2001; accepted 30 November 2001*)

Supramolecular side chain liquid crystalline polymers were prepared from poly(3-carboxypropylmethylsiloxane) (PSI100) and azobenzene-based derivatives through intermolecular hydrogen bonding between the carboxylic acid groups of PSI100 and the imidazole rings in the azobenzene-based derivatives. The presence of H-bonding was confirmed using FTIR spectroscopy. The polymeric complexes behave as liquid crystalline polymers and exhibit nematic mesophases identified on the basis of the observation of Schlieren textures. The mesogenic behaviour of these complexes was studied by polarizing optical microscopy and X-ray diffraction. The thermal behaviour of the complexes was investigated by differential scanning calorimetry. On increasing the spacer length, the transition temperatures initially increase. A further increase in spacer length, however, leads to a decrease in the transition temperatures. The electron donor–acceptor interaction between unlike mesogenic units in supramolecular copolymeric complexes helps to stabilize the mesophase.

1. Introduction

In recent years side chain liquid crystal polymers (SCLCPs), which combine properties characteristic of polymers with those of conventional low molar mass mesogens have received much attention because of their potential importance in technological applications [1–12]. Copolymerization of unlike mesogenic monomers offers a versatile means by which to control the properties of the material. A statistical distribution of the unlike mesogenic units along the copolymer backbone results in properties that are different from those of the corresponding homopolymers. The induction of smectic phases and the enhancement in the thermal stability of the mesophase are well known in copolymers made from monomers capable of exhibiting a specific interaction such as an electron donor–acceptor interaction [13–18]. The copolymers have considerable application potentials in various fields, such as information storage, nonlinear optics and electro-optic devices [19–23].

Instead of linking the pendant mesogenic units covalently to the polymer backbone, the self-assembly of the polymer through specific interactions such as hydrogen bonding (H-bonding) [24–29], ionic [30–32], ion–dipole [33, 34] and charge transfer interactions [35, 36] has been recognized as a new strategy for constructing SCLCPs. Because of the simplicity of their preparation, these self-assembled SCLCPs have the advantage of fine tunability of their liquid crystalline properties. Various molecular parameters, such as the nature of the rigid core, the nature and length of the terminal groups and the spacer length can be modified with relative ease compared with covalently-bonded systems.

H-bonding is one of the most important and widely used non-covalent interactions in the design and construction of supramolecular architectures. One advantage of hydrogen-bonded liquid crystalline polymers is the ease of preparation of various 'copolymers'. Thus, copolymers of any desired composition can be prepared by the self-assembly of a H-bonding donor polymer with a mixture of two or more different H-bonding acceptors. The LC behaviour of the copolymer can be controlled by varying the composition of the H-bonding acceptors. Although the electron donor–acceptor interaction is of importance in the development of mixtures of low molar mass liquid crystals and in the design of liquid crystalline copolymers, it has rarely been used in the design of supramolecular SCLCPs.

In the present study, we have selected a carboxylic acid-containing polysiloxane, poly(3-carboxypropylsiloxane), as the H-bonding donor polymer. The self-assembly of azobenzene-based derivatives along the polysiloxane was investigated by differential scanning calorimetry (DSC), polarizing optical microscopy (POM) and X-ray diffraction (XRD). The effect of the electron

*Author for correspondence; e-mail: chmgohsh@nus.edu.sg

Liquid Crystals ISSN 0267-8292 print/ISSN 1366-5855 online © 2002 Taylor & Francis Ltd
http://www.tandf.co.uk/journals
DOI: 10.1080/02678290210126040

donor–acceptor interaction between unlike mesogenic units on the thermal stability of the supramolecular complexes was studied.

2. Experimental

2.1. *Characterization*

^{1}H NMR spectra were recorded on a Bruker ACF 300 spectrometer at 25°C with TMS as an internal standard.

FTIR spectra were recorded on a Bio-Rad 165 FTIR spectrophotometer; 64 scans were signal-averaged with a resolution of 2 cm^{-1}. Samples were prepared by dispersing the complexes in KBr and compressing the mixtures to form disks. Spectra were recorded at a specific temperature, using a SPECAC high temperature cell equipped with an automatic temperature controller mounted in the spectrophotometer.

DSC measurements were performed using a TA Instruments 2920 differential scanning calorimeter equipped with an auto-cool accessory and calibrated using indium. The following protocol was used for each sample: heating from room temperature to 150°C at 20°C min^{-1}, holding at 150°C for 3 min, cooling from 150 to −30°C at 10°C min^{-1} and finally reheating from −30 to 150°C at 10°C min^{-1}. Data were collected during the second heating run and the first cooling run. Transition temperatures were taken as peak maxima.

The mesophase textures of the complexes and the azobenzene-based derivatives were observed under an Olympus BX50 polarizing optical microscope equipped with a Linkam THMS-600 hotstage which was controlled by a central processor. The software used in the processing of images is Image-pro plus 3.0. The sample was pressed between a glass slide and a cover slip and observed in the LC temperature range. The heating/cooling rate was 2°C min^{-1}.

XRD measurements were carried out using a Simens D5005 Diffractometer (40 kV, 30 mA) using Ni-filtered CuK_α radiation in 0.01° steps from 1.5° to 40° (in 2θ) with 1 s per step. The intensity of the diffracted X-ray from the samples was measured by a scintillation counter. The samples were annealed by heating to their isotropization temperatures followed by cooling to specific temperatures gradually prior to XRD studies. Bragg's equation was used to calculate the layer order spacing corresponding to the various reflections.

2.2. *Materials*

(3-Cyanopropyl)methyldichlorosilane, *p*-nitroaniline, aniline, imidazole and phenol were supplied by Fluka Chemika-Biochemika Company. Poly(dimethylsiloxane) (PDMS) with a viscosity of 60 000 cSt, *p*-anisidine, 4-aminobenzonitrile, 1,8-dibromo-octane, 1,6-dibromohexane, 1,4-dibromobutane and potassium carbonate were supplied by Aldrich Chemical Co. All the chemicals were used as received. Tetrahydrofuran (THF) was dried by heating under reflux with sodium in a nitrogen atmosphere. Acetone was dried over molecular sieves (4 Å).

2.3. *Synthesis of carboxylic acid-containing polysiloxane*

The synthesis and characterization of PSI100 have been reported elsewhere [37]. PSI100 shows an initial decomposition temperature at 210°C, as shown by thermogravimetric analysis. The number-average molecular weight of PSI100 is 6.6 kg mol^{-1} and the polydispersity is 1.6. The glass transition temperature of PSI100 is −9°C.

2.4. *Synthesis of 4-hydroxy-4′-cyanoazobenzene*

4-Aminobenzonitrile (17.7 g, 0.15 mol) was dissolved in warm hydrochloric acid (6M, 100 ml). Ice (200 g) was added and the solution was cooled to 0–5°C in an ice-water bath. To this solution was slowly added a cold solution of sodium nitrite (11.7 g, 0.17 mol) in distilled water (80 ml) with vigorous stirring. The resulting diazonium salt solution was then slowly added to a stirred solution of phenol (14.1 g, 0.15 mol) in 10% aqueous sodium hydroxide (145 ml) at 0–5°C. The reaction mixture was stirred for 30 min and then acidified with concentrated hydrochloric acid. The resulting precipitate was washed with copious amounts of water and dried under vacuum. The crude product was purified on a silica gel column using ethyl acetate/hexane (1/3) as the eluent. ^{1}H NMR ($CDCl_3$, ppm): 7.93–7.97 (4H, N=N−Ar−H), 7.78–7.81 (2H, CN−Ar−H), 6.96–6.99 (2H, O−Ar−H). Anal: calcd for $C_{13}H_9N_3O$ C 69.96, H 4.04, N 18.83; found C 69.78, H 4.22, N 18.54%.

2.5. *Synthesis of 1-bromo-6-(4-cyanoazobenzene-4′-oxy)hexane*

A mixture of 4-hydroxy-4′-cyanoazobenzene (6.7 g, 0.03 mol), 1,6-dibromohexane (14.6 g, 0.06 mol), potassium carbonate (4.8 g, 0.035 mol) and dry acetone (100 ml) was heated at reflux for 24 h in a nitrogen atmosphere. The reaction mixture was filtered hot and the residue washed with acetone. The filtrate was concentrated by evaporation. A crystalline product was obtained by adding a large amount of cold hexane. The crude product was recrystallized from cold hexane and dried in vacuum. ^{1}H NMR ($CDCl_3$, ppm): 7.94–7.99 (4H, N=N−Ar−H), 7.78–7.81 (2H, CN−Ar−H), 7.00–7.04 (2H, O−Ar−H), 4.05–4.10 (2H, Ar−O−CH_2), 3.43–3.49 (2H, Br−CH_2), 1.86–1.97 (4H, Ar−O−C−CH_2, Br−C−CH_2), 1.52–1.56 (4H, Br−C−C−CH_2CH_2−C−C−O). Anal: calcd for $C_{19}H_{20}N_3OBr$ C 59.07, H 5.18, N 10.88; found C 58.79, H 5.25, N 11.03%.

2.6. *Synthesis of 4-cyano-4′-[6-(imidazole-1-yl)-hexyloxy]azobenzene (CN6I)*

A mixture of 1-bromo-6-(4-cyanoazobenzene-4′-oxyl)-hexane (3.9 g, 0.01 mol), imidazole (1.0 g, 0.015 mol) and potassium carbonate (2.8 g, 0.02 mol) in dry THF (100 ml) was heated at reflux with stirring for 24 h under a nitrogen atmosphere. After the addition of dichloromethane (100 ml), the solution was filtered to remove salts. After the removal of THF and dichloromethane, the crude product was purified on a silica gel column using dichloromethane/methanol (30/1) as eluent. ^{1}H NMR ($CDCl_3$, ppm): 7.93–7.98 (4H, N=N−Ar−H), 7.77–7.79 (2H, CN−Ar−H), 7.01–7.05 (2H, O−Ar−H), 7.47, 7.06, 6.91 (3H, imidazolyl), 4.03–4.07 (2H, Ar−O−CH_2), 3.94–3.98 (2H, Im−CH_2), 1.79–1.86 (4H, Ar−O−C−CH_2, Im−C−CH_2), 1.51–1.56 (2H, Im−C−C−C−CH_2−C−C−O), 1.36–1.44 (2H, Im–C–C–CH_2–C–C–C–O–Ar). Anal: calcd for $C_{22}H_{23}N_5O$ C 70.78, H 6.17, N 18.77; found C 71.00, H 6.42, N 18.59%.

4-Cyano-4′-[4-(imidazole-1-yl)butyloxy]azobenzene (CN4I), 4-cyano-4′-[8-(imidazole-1-yl)octyloxy]azobenzene (CN8I), 4-nitro-4′-[6-(imidazole-1-yl)hexyloxy]azobenzene (NO6I), 4-methoxy-4′-[6-(imidazole-1-yl)hexyloxy]azobenzene (MEO6I), 4-methoxy-4′-[4-(imidazole-1-yl)butyloxy]azobenzene (MEO4I), and 4-[6-(imidazole-1-yl)hexyloxy]azobenzene (H6I) were similarly prepared.

2.7. *Preparation of hydrogen-bonded complexes*

All hydrogen-bonded complexes were prepared by solution casting using THF as solvent. The complete removal of THF was ensured, initially by slow evaporation at room temperature followed by drying *in vacuo* for two weeks at 60°C. Unless otherwise stated, the complex contained an equimolar ratio of carboxylic acid and imidazole groups.

'Copolymeric' complexes were prepared using PSI100 and two different azobenzene-based derivatives by maintaining a 1 : 1 stoichiometry between the carboxylic acid groups in PSI100 and the imidazole groups in the mixture of the different azobenzene-based derivatives.

3. Results and discussion

3.1. *Formation of side chain liquid crystalline polymers through hydrogen bonding*

The structures of the side chain liquid crystalline polymers (SCLCPs) formed through H-bonding between the carboxylic acid groups in PSI100 and the imidazole rings in azobenzene-based derivatives are shown in the scheme.

Figure 1 shows the DSC results of pure CN6I and its complexes with PDMS or PSI100 using a functional group feed ratio of 1 : 1. The transition temperatures and the associated enthalpy changes (ΔH) are listed in table 1. In the cooling run of CN6I, only one exothermic peak arising from crystallization is observed at 75°C with an enthalpy change of 32.34 kJ mol^{-1}, while on heating, the endothermic peak at 120°C ($\Delta H = 35.02$ kJ mol^{-1}) is ascribed to the melting of CN6I into the isotropic phase. The results of the POM study and XRD measurements, which will be discussed later, confirm this assignment. The difference between the crystallization and melting temperatures is due to supercooling. The PDMS/CN6I mixture shows similar phase transition behaviour to that of pure CN6I. An exothermic peak at 64°C with an enthalpy change of 18.64 kJ mol^{-1} and an endothermic

Scheme

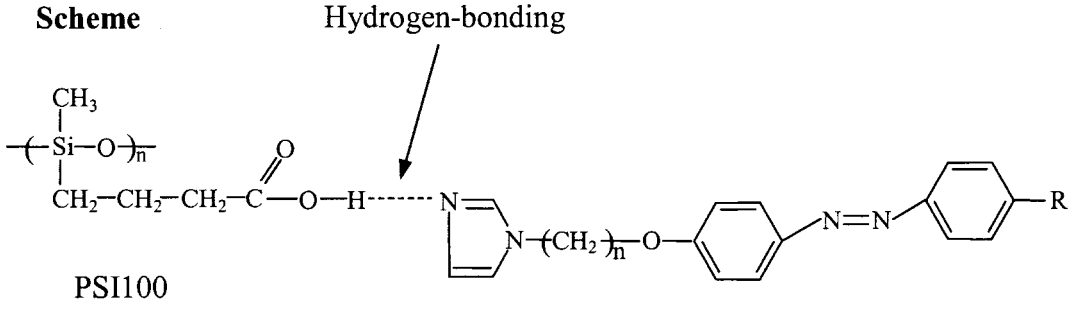

CN4I, n = 4, R = CN; CN6I, n = 6, R = CN;
CN8I, n = 8, R = CN; MEO4I, n = 4, R = OCH_3;
MEO6I, n = 6, R = OCH_3; NO6I, n = 6, R = NO_2;
H6I, n = 6, R = H;

Scheme.

Table 1. Transition temperatures (°C) and associated enthalpy changes (kJ mol^{-1}, in parentheses) of CN6I and its complexes: I = isotropic phase, Cr = crystalline phase, N = nematic phase, g = glassy phase.

	1st cooling	2nd heating
CN6I	I 75(32.34) Cr	Cr 120(35.02) I
PDMS/CN6I	I 64(18.64) Cr	Cr 118(22.59) I
PSI100/CN6I	I 68(1.12) N 43(16.16) Cr	g 9 Cr_1 57(3.83) Cr_2 88(2.24) Cr_3 101(16.06) I

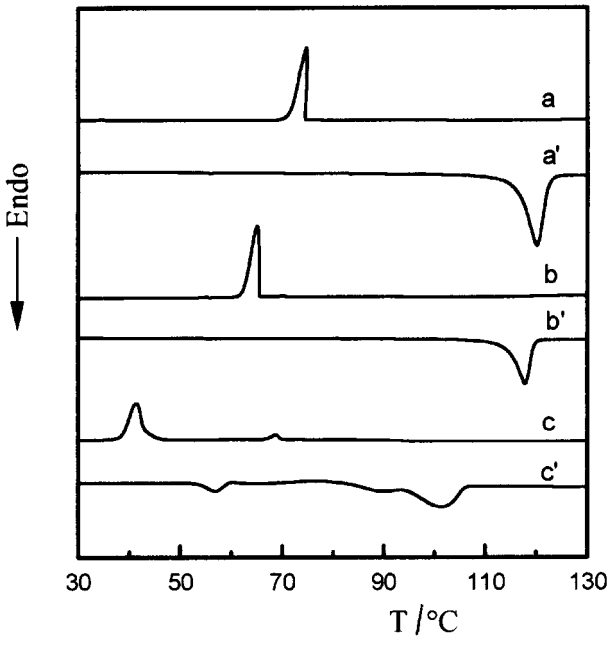

Figure 1. DSC traces of CN6I and its complexes. First cooling run: (a) CN6I, (b) PDMS/CN6I, (c) PSI100/CN6I; second heating run: (a′) CN6I, (b′) PDMS/CN6I, (c′) PSI100/CN6I.

peak at 118°C with an enthalpy change of 22.59 kJ mol^{-1} are observed in the first cooling run and the second heating run, respectively. The production in the transition temperatures arises from the disrupting effect of the PDMS chains on the degree of order in the crystal. Birefringent behaviour is not found for the mixture below the transition temperature under POM. The similar thermal behaviour of CN6I and the PDMS/CN6I mixture indicates the absence of any specific interaction between CN6I and PDMS.

Curves c and c′ in figure 1 are the DSC curves of the PSI100/CN6I complex for the first cooling run and second heating run, respectively. Compared to pure CN6I and the PDMS/CN6I mixture, an exothermic peak at 68°C (T_{IN}) with an enthalpy change of 1.12 kJ mol^{-1} is observed in the cooling run, corresponding to the transition from the isotropic state to a liquid crystalline phase. On further cooling, a peak due to the crystallization of the complex from the mesophase appears at 43°C (T_{NCr}) with an enthalpy change of 16.16 kJ mol^{-1}. There are three endothermic peaks at 57, 88 and 101°C in the second heating run; these are ascribed to the melting of different crystalline phases. POM and XRD measurements show that the complex shows a nematic phase in the temperature range from T_{IN} to T_{NCr} in the first cooling run but no birefringent behaviour was observed in the second heating run. Thus, the DSC data indicate that the PSI100/CN6I complex prepared from two different non-mesogenic components behaves as a single mesogenic compound. The intermolecular H-bonding between the imidazole ring in CN6I and the carboxylic acid group on PSI100 gives rise to a supramolecular SCLCP exhibiting a monotropic nematic phase. The monotropic behaviour is due to the melting temperature of the crystal being higher than the nematic–isotropic transition temperature.

The formation of intermolecular H-bonding is supported by FTIR measurements, which suggests that the acid dimer is replaced by the complex in PSI100. Specifically, on mixing PSI100 with CN6I, the broad carbonyl stretch at around 1710 cm^{-1} becomes sharper and the peak maximum moves to a higher wavenumber. The changes are consistent with the liberation of carbonyl groups from the carboxylic acid dimer. In addition, Fermi resonance bands at 2620 and 1930 cm^{-1} become more apparent. These are observed when an acid is hydrogen-bonded to a base [38].

On cooling the PSI100/CN6I complex from the isotropic phase, a birefringent texture develops when viewed through the polarizing microscope. In order to obtain a clear characteristic optical texture for phase identification, the complex was cooled slowly from approximately 20°C above its isotropization temperature at 2°C min^{-1} prior to analysis. The optical texture observed under crossed polarizers is shown in figure 2. For CN6I, on cooling from the isotropic phase, a spherical texture typical of a crystal formed quickly at 76°C and no further change was observed on cooling. Thus CN6I does not show mesophasic behaviour. In contrast, for the PSI100/CN6I complex, a Schlieren texture formed slowly at 69°C on cooling from the isotropic phase, see figure 2. Thus, the mesophase exhibited by the complex is assigned as a nematic phase. These results clearly demonstrate that a new nematic SCLCP has been constructed through intermolecular H-bonding.

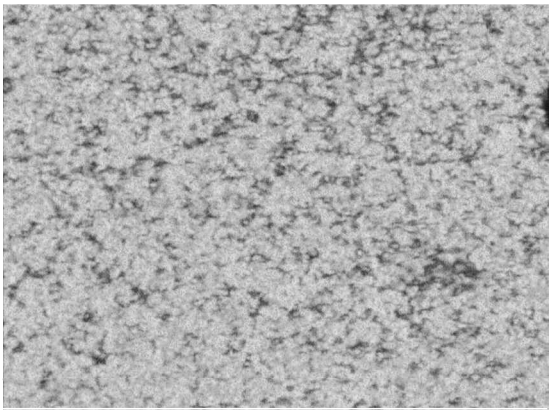

Figure 2. Optical micrographs of the PSI100/CN6I complex (magnification 400×).

In order to confirm the molecular order and to ascertain the morphology of the liquid crystalline texture of the complex, XRD studies were carried out. Figure 3 presents the XRD patterns of CN6I and the PSI100/CN6I complex. At room temperature, the existence of several sharp peaks in the low and high angle regions indicates a crystal phase for CN6I, figure 3(*a*). The low angle region maxima are due to a layer-like structure, and the sharp high angle maxima indicate an ordered structure within the layer. Compared with the XRD pattern of CN6I, there is a significant change in the XRD pattern of the PSI100/CN6I complex at 55°C. The XRD pattern of the PSI100/CN6I complex does not contain sharp peaks in either the low or the high angle region; instead, a diffuse halo at 20.9° corresponding to a d value of 4.2 Å was observed. This result indicates that the PSI100/CN6I complex exhibits a nematic mesophase. In the nematic phase, $d = 4.2$ Å corresponds to the average distance between the mesogenic units.

3.2. *Effects of complex composition and spacer length*

To determine compositional effects on the mesophasic properties of these supramolecular assemblies, a number of PSI100/CN6I complexes of varying composition were prepared. The complexes were miscible over the whole composition range as judged by POM. Figure 4 shows the DSC curves of the first cooling run and the second heating run of the various PSI100/CN6I complexes. The corresponding transition temperatures and enthalpy changes of the complexes are shown in table 2. As shown in figure 4 and table 2, on increasing the concentration of CN6I, T_{IN} and the associated ΔH increase initially until the feed ratio of CN6I to PSI100 reaches 1:1, and then decrease on further addition of CN6I. The formation of these supramolecular SCLCPs is due to the assembly of low-molar-mass compounds and the polymer backbone through H-bonding between the carboxylic acids

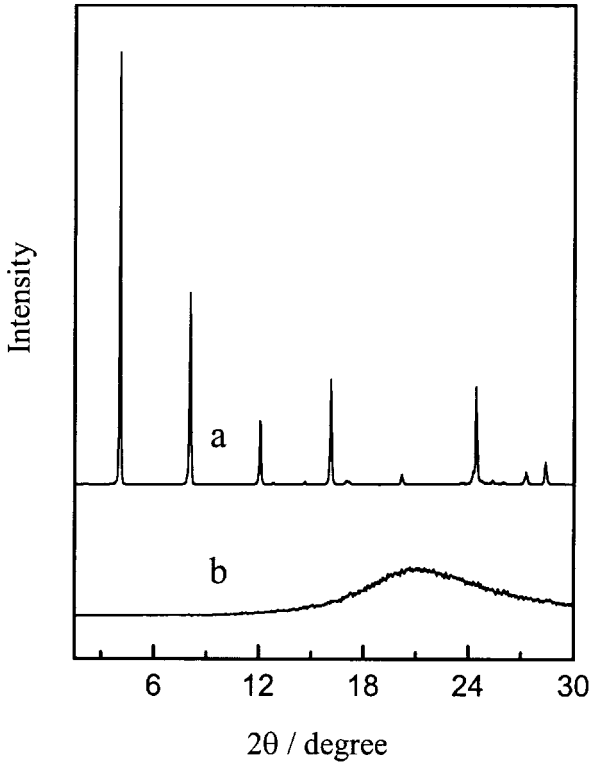

Figure 3. XRD patterns of (*a*) CN6I at 25°C and (*b*) the complex PSI100/CN6I at 55°C.

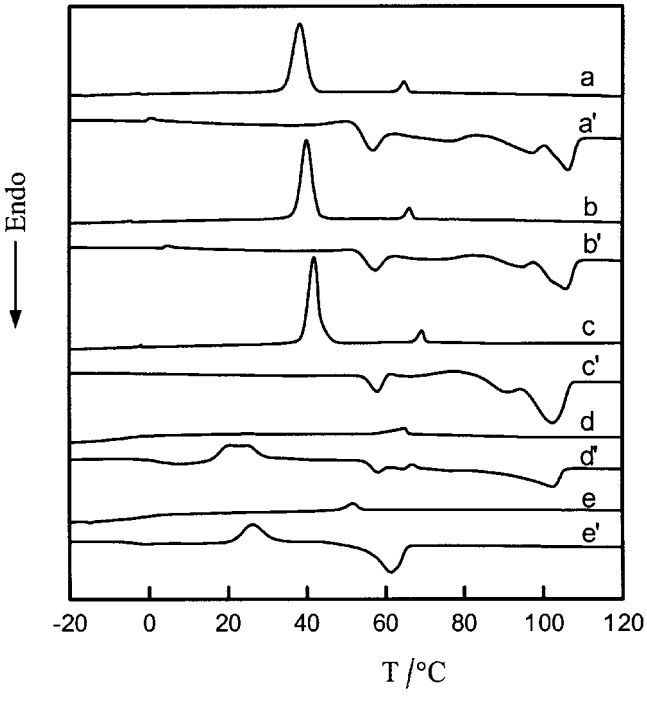

Figure 4. DSC traces of PSI100/CN6I complexes of different molar ratios. First cooling run: (a) 1:1.4, (b) 1:1.2, (c) 1:1, (d) 1:0.8, (e) 1:0.6; second heating run: (a′) 1:1.4, (b′) 1:1.2, (c′) 1:1, (d′) 1:0.8, (e′) 1:0.6.

Table 2. Transition temperatures (°C) and associated enthalpy changes (kJ mol^{-1}, in parentheses) of PSI100/CN6I complexes of varying composition: I = isotropic phase, Cr = crystalline phase, Cr^c = cold crystallization, N = nematic phase, g = glassy phase.

Mol ratio (PSI100 : CN6I)	1st cooling	2nd heating
1 : 0.6	I 52(0.51) N	g −5 Cr^c 26(7.18) Cr 61(13.05) I
1 : 0.8	I 64(0.77) N	g 2 Cr$_1^c$ 19(0.16) Cr$_2^c$ 24(2.28) Cr$_1$ 57(0.69) Cr$_2$ 64(0.38) Cr$_3$ 102(7.95) I
1 : 1.0	I 68(1.12) N 43(16.16) Cr	g 9 Cr$_1$ 57(3.83) Cr$_2$ 88(2.24) Cr$_3$ 101(16.06) I
1 : 1.2	I 65(0.95) N 40(19.95) Cr	g 7 Cr$_1$ 57(5.62) Cr$_2$ 93(2.56) Cr$_3$ 105(11.98) I
1 : 1.4	I 63(0.82) N 38(21.84) Cr	g 6 Cr$_1$ 56(5.78) Cr$_2$ 97(2.83) Cr$_3$ 106(6.64) I

groups in PSI100 and the imidazole rings in CN6I. The connection of the mesogenic unit to the polymer backbone increases the stiffness of the polymer backbone, and restricts the movement of the mesogenic units facilitating the packing of the mesogenic units along a specific direction. As a result, the clearing temperature increases with increasing feed ratio of CN6I to PSI100. The increase in the stiffness of the polymer backbone is shown by the change of T_g from −5°C with a molar ratio of 0.6 to 9°C with a molar ratio of 1.0. Alternatively, the various PSI100/CN6I complexes can be regarded as copolymers of the H-bonded mesogenic unit CN6I and the non-mesogenic unit containing the carboxylic acid group. As the carboxylic acid group does not show mesogenic behaviour, it plays the role of a 'diluent' in the LC phase of the complex, leading to a decrease in the mesophase thermal stability. As a result, increasing the concentration of the carboxylic acid group will lead to a decrease in T_{IN}. The formation of a SCLCP at the molar ratio of 0.6 indicates that the H-bonded CN6I at such a level is sufficient for the formation of a mesophase.

We have studied the thermal stability of the PSI100/NO6I complex of varying composition and found the minimum molar ratio necessary for the formation of a LC phase is 0.4 [39]. The lower minimum ratio for the PSI100/NO6I complex is due to the stronger polar interactions between NO6I than between CN6I. When the molar ratio of PSI100 to CN6I is 1 : 1.2 or higher, there are insufficient carboxylic acid groups to interact with CN6I in a one to one manner. As a result, some CN6I cannot be arranged along the polymer backbone through H-bonding. Although this excess can be incorporated into the LC phase through the intermolecular interaction between the CN6I molecules, it disrupts the ordering of the phase, and the transition temperature and enthalpy change decrease.

For SCLCPs, the spacer between the polymer backbone and the mesogenic side group plays an important role in determining the LC behaviour of the polymer. The function of the spacer is to decouple the motions of the polymer backbone (which tends to form a random coil) from those of the mesogenic groups which are ordered in the liquid crystal phase. Generally, an increase in spacer length results in an increase of the I–N transition temperature. Figures 5 and 6 show the DSC curves of the first cooling run and the second heating run of PSI100/CN4I, PSI100/CN6I and PSI100/CN8I complexes at a feed ratio of 1 : 0.8 or 1 : 1, respectively. The corresponding transition temperatures and the enthalpy changes of the complexes are listed in table 3. The difference between CN4I, CN6I and CN8I is the chain length between the imidazole group and the azobenzene group. As a result, the spacer length in the supramolecular complexes increases from the PSI100/CN4I complex to the PSI100/CN6I complex and to the PSI100/CN8I complex. As shown in figure 5 and table 3, the phase transition temperature (T_{IN}) and the enthalpy change (ΔH) increase from 42°C and 0.65 kJ mol^{-1} for the PSI100/CN4I complex to 64°C and 0.77 kJ mol^{-1} for the PSI100/CN6I complex at the feed ratio of 0.8.

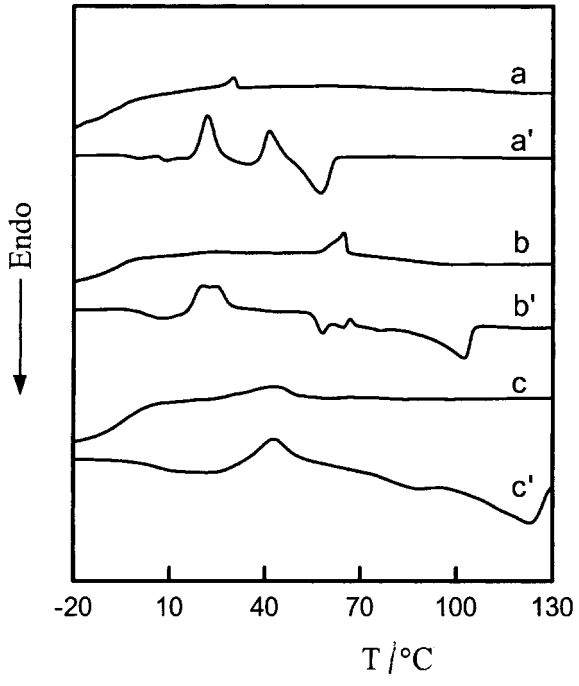

Figure 5. DSC traces of various complexes at feed ratio of 1 : 0.8. First cooling run: (a) PSI100/CN8I, (b) PSI100/CN6I, (c) PSI100/CN4I; second heating run: (a′) PSI100/CN8I, (b′) PSI100/CN6I, (c′) PSI100/CN4I.

Table 3. Transition temperatures (°C) and associated enthalpy changes (kJ mol^{-1}, in parentheses) of various complexes at a feed ratio of 1 : 1 or 1 : 0.8: I = isotropic phase, Cr = crystalline phase, Cr^c = cold crystallization, N = nematic phase, g = glassy phase.

	Mol ratio	1st cooling	2nd heating
PSI100/CN4I	1 : 0.8	I 42(0.65) N	g 7 Cr^c 43(13.22) Cr 123(12.92) I
	1 : 1	I 46(0.70) N	g 12 Cr^c 60(5.49) Cr 94(4.20) I
PSI100/CN6I	1 : 0.8	I 64(0.77) N	g 2 Cr_1^c 19(0.16) Cr_2^c 24(2.28) Cr_1 57(0.69) Cr_2 64(0.38) Cr_3 102(7.95) I
	1 : 1	I 68(1.12) N 43(16.16) Cr	g 9 Cr_1 57(3.83) Cr_2 88(2.24) Cr_3 101(16.06) I
PSI100/CN8I	1 : 0.8	I 30(0.29) N	g −3 Cr_1^c 21(11.85) Cr_2^c 40(8.78) Cr 56(10.50) I
	1 : 1	I 43(0.38) N 19(1.82) Cr	g −6 Cr_1^c 8(0.34) Cr_2^c 14(5.24) Cr_3^c 38(4.70) Cr 58(17.84) I

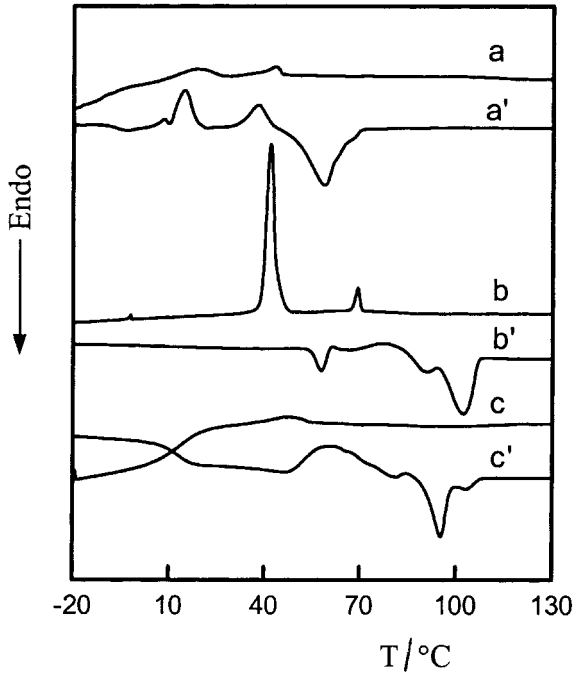

Figure 6. DSC traces of various complexes at feed ratio of 1 : 1. First cooling run: (a) PSI100/CN8I, (b) PSI100/CN6I, (c) PSI100/CN4I; second heating run: (a′) PSI100/CN8I, (b′) PSI100/CN6I, (c′) PSI100/CN4I.

Thus, an increase in the spacer length by two methylene units leads to an increase in the thermal stability of the LC phase. However, T_{IN} and ΔH decrease from 64°C and 0.77 kJ mol^{-1} for the PSI100/CN6I complex to 30°C and 0.29 kJ mol^{-1} for the PSI100/CN8I complex at the feed ratio of 0.8. This indicates that further increase of the spacer length decreases the thermal stability of the LC phase. The longer spacer apparently increases the flexibility of the side chain. Similar results have been observed for the complexes at feed ratio of 1. On increasing the spacer length from four to eight methylene units, the T_gs of the complexes decrease from 7°C and 12°C to −6°C and −3°C at the feed ratios 0.8 and 1, respectively. The decrease of T_g is due to the increase of the decoupling function of the spacer with increasing length.

3.3. *Effect of electron donor–acceptor interaction*

Figure 7 shows the phase diagram of PSI100/(CN6I-MEO6I) complexes derived from PSI100 and a mixture of CN6I and MEO6I, in which the complexes are formed based on a 1 : 1 stoichiometry of the H-bonding donor and acceptor groups. The copolymeric complexes exhibit characteristic phase transitions and homogeneous mesophases over the entire composition range. As shown in figure 7, the I–N transition temperatures of the copolymeric complexes show a significant positive deviation. Thus all the copolymeric PSI100/(CN6I-MEO6I) complexes exhibit thermal stabilization and wide temperature ranges of the mesophase. CN6I possesses an electron-withdrawing terminal group, and MEO6I carries an electron-donating terminal group. In consequence, there exists a type of electron donor–acceptor interaction between MEO6I and CN6I. The thermal stabilization

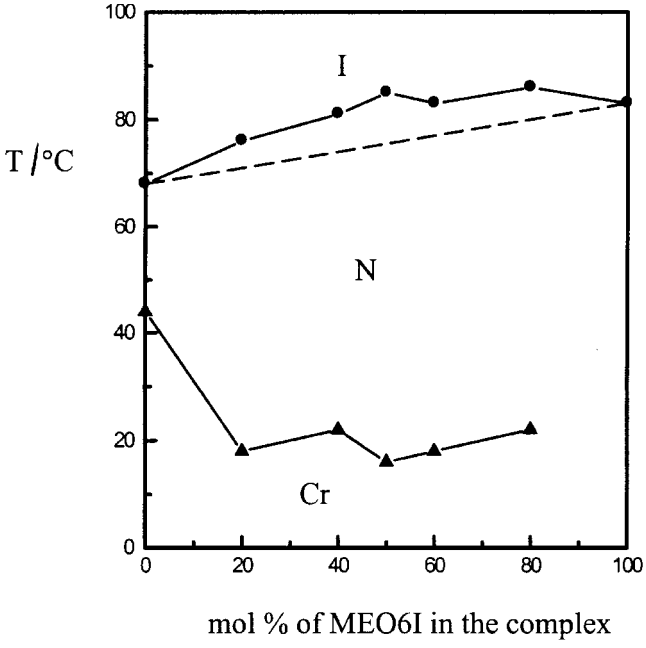

Figure 7. Phase diagram of the PSI100/(CN6I-MEO6I) system: I = isotropic phase, N = nematic phase, Cr = crystalline phase.

of the mesophase in the self-assembled H-bonded copolymeric PSI100/(CN6I-MEO6I) complexes is attributed to this electron donor–acceptor interaction.

A similar result is observed for the copolymeric PSI100/(CN4I-MEO4I) complexes, as shown in figure 8, except that a significant positive deviation in T_{IN} is only observed when the MEO4I content is between 40 and 80 mol %. This is due to the reduced strength of the electron donor–acceptor interaction in the PSI100/(CN4I-MEO4I) complexes compared with that in the PSI100/(CN6I-MEO6I) complexes. The strength of electron donor–acceptor interaction is determined by the degree of overlap between the unlike mesogenic units [17, 40]. The existence of the bulky imidazole group in the spacer disturbs the overlap of the unlike mesogenic units, and it becomes larger on decreasing the chain length between the imidazole group and the mesogenic unit. As a result, the positive deviation of the transition temperatures is smaller in the copolymeric PSI100/(CN4I-MEO4I) complex than in the PSI100/(CN6I-MEO6I) complexes.

The disrupting effect of the imidazole groups on the overlap of unlike mesogenic units is a view supported by the DSC results of the analogous low molar mass compounds. Figure 9 shows the DSC curves of the first cooling runs of CN6I, CN4I, MEO6I, MEO4I and the binary mixtures CN6I/MEO6I and CN4I/MEO4I. There is only one exothermic peak at 111 and 50°C in the first cooling run of CN4I and MEO4I, respectively.

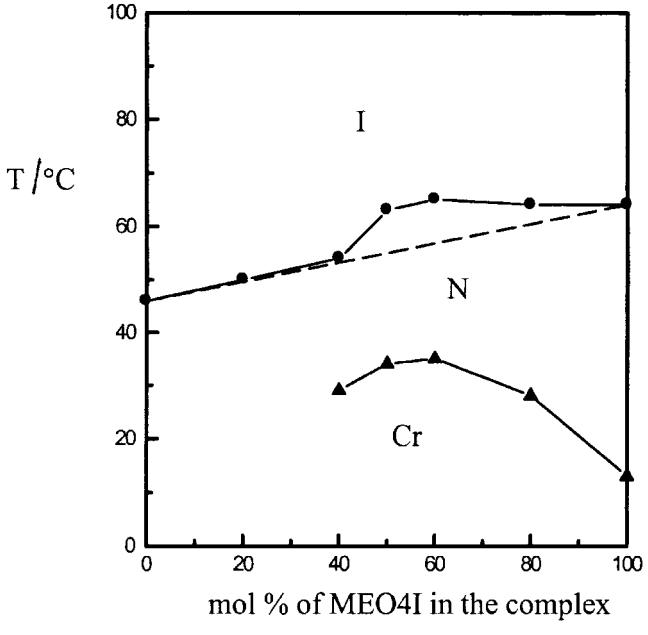

Figure 8. Phase diagram of the PSI100/(CN4I-MEO4I) system: I = isotropic phase, N = nematic phase, Cr = crystalline phase.

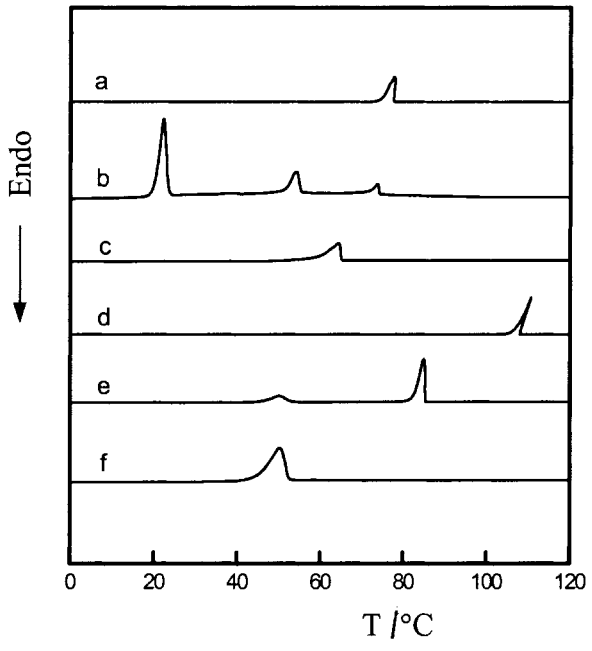

Figure 9. DSC traces of the first cooling run: (a) CN6I, (b) CN6I/MEO6I, (c) MEO6I, (d) CN4I, (e) CN4I/MEO4I, (f) MEO4I.

Based on POM observations and XRD measurements, these peaks are associated with crystallization from the isotropic phase. The binary CN4I/MEO4I mixture shows two exothermic peaks at 85 and 50°C, corresponding to the crystallization temperatures of CN4I and MEO4I, respectively. The reduction of the crystallization temperature of CN4I is due to the disrupting effect of MEO4I on the ordering of CN4I molecules. The POM results indicate that the binary CN4I/MEO4I mixture exhibits no mesogenic behaviour, but phase separation occurs. This indicates that the bulky imidazole group prevents the overlapping of the unlike units, and no apparent electron donor–acceptor interaction was observed in the binary mixture. By constrast, there are three exothermic peaks in the first cooling run of the binary CN6I/MEO6I mixture. The peaks at 73 and 55°C correspond to the crystallization of pure CN6I at 76°C and pure MEO6I at 65°C, respectively, while the appearance of a new peak at 23°C is due to the specific electron donor–acceptor interaction between the unlike units, and a new kind of crystal phase is formed. The POM results indicate that the binary CN6I/MEO6I mixture exhibits no mesogenic behaviour, but phase separation occurs. It is noteworthy, however, that the electron donor–acceptor interaction in the binary CN6I/MEO6I mixture is stronger than that in the binary CN4I/MEO4I mixture. The chain length between the imidazole group and the azobenzene group in CN4I or MEO4I is shorter than that in CN6I or MEO6I, and thus the disrupting

effect of the bulky imidazole group on the electron donor–acceptor interaction is greater in the binary CN4I/MEO4I mixture than in the CN6I/MEO6I mixture.

Imrie *et al.* [41] have reported the DSC results of NABO6 and MEOABO6 having similar structures to those of NO6I and MEO6I except that the terminal group is hydrogen instead of imidazole. They found that NABO6 and MEOABO6 exhibit a mesophase (nematic or smetic) and attributed the thermal enhancement of the phase in the binary NABO6/MEOABO6 mixture to the electron donor–acceptor interaction between the unlike units. The difference between their results and those presented here is the disrupting effect of the bulky imidazole group on the ability of unlike mesogenic units to overlap in our system which prevents mesophase formation.

Copolymeric PSI100/(CN6I-NO6I) complexes were prepared by complexing PSI100 with a mixture of CN6I and NO6I while maintaining a 1 : 1 overall stoichoimetry of the H-bonding donor and acceptor moieties. A phase diagram for the complexes is shown in figure 10, and the phase transition temperatures of the copolymeric complexes show a negative deviation from ideal behaviour, i.e. the temperatures are lower than those of the corresponding homopolymeric PSI100/CN6I and PSI100/NO6I complexes. Both CN6I and NO6I have electron-withdrawing terminal groups and thus there is no electron donor–acceptor interaction between CN6I and the NO6I. However, in the copolymeric complexes, CN6I disrupts the interactions between NO6I, and likewise NO6I between CN6I. As a result, the phase transition temperatures show a negative deviation and are lower than those of the corresponding homopolymeric complex. The transition temperatures and corresponding enthalpy changes shown in table 4 also reveal the decrease of the thermal stability of copolymeric PSI100/(CN6I-NO6I) complexes. This result provides additional evidence in support of the earlier conclusion that electron donor–acceptor interactions play an important role in the thermal stability of these copolymeric complexes containing electron donor and electron acceptor mesogenic units.

In copolymers containing a statistical distribution of mesogenic side chains and non-mesogenic side chains along the polymer backbone, it is assumed that the non-mesogenic groups would largely prevent the intermolecular association of the mesogenic groups. As a result, the mesogenic properties of the polymer can be adjusted through copolymerization. In the same way, the mesogenic properties of supramolecular copolymeric complexes can also be adjusted through the formation of copolymeric complexes from PSI100 and a mixture of two kinds of low molar mass compounds, whose homopolymeric complex may or may not be liquid crystalline. Figure 11 shows the phase diagram of the self-assembled copolymeric PSI100/(CN6I-H6I) complex, while maintaining a 1 : 1 overall stoichiometry of the H-bonding donor and acceptor moieties. Although the crystalline phase was formed in the first cooling run of the PSI100/CN6I complex, there was no crystalline phase observed for the copolymeric PSI100/(CN6I-H6I) complex. On increasing the feed ratio of H6I to CN6I, T_{IN} decreases, but the glass transition temperature shows no dependence on the feed ratio. As reported earlier [39], the PSI100/H6I complex is not liquid crystalline which is in accord with the well known fact that the hydrogen atom lies low in the order of terminal substituents promoting

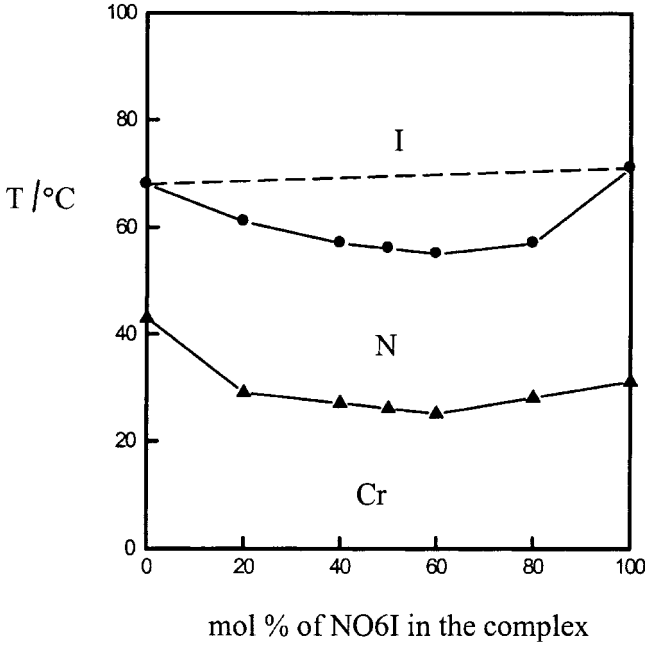

Figure 10. Phase diagram of the PSI100/(CN6I-NO6I) system: I = isotropic phase, N = nematic phase, Cr = crystalline phase.

Table 4. Transition temperatures (°C) and associated enthalpy changes (kJ mol^{-1}, in parentheses) of copolymeric PSI100/(CN6I-NO6I) complexes: I = isotropic phase, N = nematic phase, Cr = crystalline phase.

Mol fraction of NO6I /mol %	Transitions
0	I 68(1.12) N 43(16.16) Cr
20	I 61(1.05) N 29(10.30) Cr
40	I 57(1.13) N 27(9.06) Cr
50	I 56(0.92) N 26(9.25) Cr
60	I 55(0.98) N 25(9.04) Cr
80	I 57(1.11) N 28(9.04) Cr
100	I 71(1.43) N 31(9.07) Cr

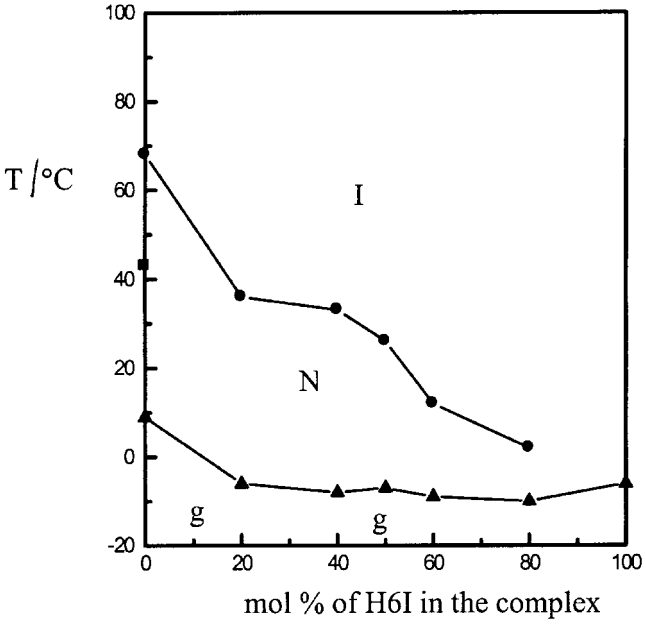

Figure 11. Phase diagram of the PSI100/(CN6I-H6I) system: I = isotropic phase, N = nematic phase, g = glassy phase.

liquid crystal properties relative to the methoxy, nitro and cyano groups. The presence of H6I in the copolymeric complexes, prevents the association of the CN6I units in the complexes and the copolymer shows lower transition temperatures. The minimum concentration of CN6I necessary for the formation of the nematic phase in the PSI100/(CN6I-H6I) complex is 20 mol %. This result further supports the earlier conclusion that electron donor–acceptor interactions play an important role in the thermal stability of mesophases formed by supramolecular copolymeric complexes.

4. Conclusions

The attachment of azobenzene-based derivatives to the polymer PSI100 through H-bonding leads to the formation of supramolecular SCLCPs as confirmed by DSC, POM, XRD and FTIR studies. The thermal stability of the mesophase initially increases with increasing spacer length, but further increases in spacer length lead to a decrease in the thermal stability. This is due to the opposing effects of the decoupling function of the spacer and the flexibility of the spacer on the thermal stability of the mesophase. The specific electron donor–acceptor interaction between unlike mesogenic units enhances the thermal stability of mesophases, while the bulky imidazole group in the spacer disrupts such interactions. The mesogenic unit concentration in the complex also affects the thermal stability of the mesophase and its temperature range.

References

[1] Abe, J., Hasegawa, M., Matsushima, H., Shirai, Y., Nemoto, N., Nagase, Y., and Takamiya, N., 1995, *Macromolecules*, **28,** 2938.
[2] Imrie, C. T., Karasz, F. E., and Attard, G. S., 1994, *Macromolecules*, **27,** 1578.
[3] Bautista, M. O., Duran, R. S., and Ford, W. T., 1993, *Macromolecules*, **26,** 659.
[4] Trollsas, M., Sahlen, F., Gedde, U. W., Hult, A., Hermann, D., Rudquist, P., Komitov, L., Lagerwall, S. T., Stebler, B., Lindstrom, J., and Rydlund, O., 1996, *Macromolecules*, **29,** 2590.
[5] Ho, M. S., Natansohn, A., and Rochon, P., 1996, *Macromolecules*, **29,** 44.
[6] Meng, X., Natansohn, A., Barretl, C., and Rochon, P., 1996, *Macromolecules*, **29,** 946.
[7] Hvilsted, S., Andruzzi, F., Kulinna, C., Siesler, H. W., and Ramanujam, P. S., 1995, *Macromolecules*, **28,** 2172.
[8] Berg, R. H., Hvilsted, S., and Ramanujam, P. S., 1996, *Nature*, **383,** 505.
[9] Zhou, W., Fu, R., Dai, R., Huang, Z., and Chen, Y., 1994, *J. Chromatogr.*, **659,** 477.
[10] Fu, R., Jing, P., Gu, J., Huang, Z., and Chen, Y., 1993, *Anal. Chem.*, **65,** 2141.
[11] Saito, Y., Jinno, K., Pesek, J. J., Chen, Y. L., Luchr, G., Archer, J., Fetzer, J. C., and Biggs, W. R., 1993, *Chromatographia*, **38,** 295.
[12] Pesek, J. J., Lu, Y., Sioux, A., and Grandperrin, F., 1991, *Chromatographia*, **31,** 147.
[13] Kodaira, T., Endo, M., and Kurachi, M., 1998, *Macromol. Chem. Phys.*, **199,** 2329.
[14] Kodaira, T., Kurachi, M., Chiou, J. Y., and Endo, M., 1999, *Macromol. Chem. Phys.*, **200,** 997.
[15] Imrie, C. T., Attard, G. S., and Karasz, F. E., 1996, *Macromolecules*, **29,** 1031.
[16] Imrie, C. T., and Paterson, B. J. A., 1994, *Macromolecules*, **27,** 6673.
[17] Imrie, C. T., and Craig, A. A., 1997, *Polymer*, **38,** 4951.
[18] Kosaka, Y., and Uryu, T., 1995, *Macromolecules*, **28,** 9295.
[19] McArdle, C. B. (editor), 1989, *Side Chain Liquid Crystal Polymers* (Glasgow: Blackie).
[20] Chapoy, L. L. (editor), 1985, *Recent Advances in Liquid Crystalline Polymers* (London: Elsevier).
[21] Smith, D. A. M., and Coles, H. J., 1993, *Liq. Cryst.*, **14,** 937.
[22] Schlech, T., Imrie, C. T., Rice, D. M., Karasz, F. E., and Attard, G. S., 1993, *J. polym. Sci. A: polym. Chem.*, **31,** 1859.
[23] Green, M. M., Ringsdort, H., Wagner, J., and Wüstefeld, R., 1990, *Angew. Chem., int. Ed. Engl.*, 1497.
[24] Kumar, U., Kato, T., and Frèchet, J. M. J., 1992, *J. Am. chem. Soc.*, **114,** 6630.
[25] Kumar, U., Frèchet, J. M. J., Kato, T., Ujiie, S., and Timura, K., 1992, *Angew. Chem. int. Ed. Engl.*, **31,** 1531.
[26] Van Nunen, J. L. M., Folmer, B. F. B., and Nolte, R. J. M., 1997, *J. Am. chem. Soc.*, **119,** 283.
[27] Kato, T., Ihata, O., Ujiie, S., Tokita, M., and Watanabe, J., 1998, *Macromolecules*, **31,** 3551.
[28] Kawakami, T., and Kato, T., 1998, *Macromolecules*, **31,** 4475.

[29] Stewart, D., and Imrie, C. T., 1997, *Macromolecules*, **30,** 877.
[30] Ujiie, S., and Limura, K., 1992, *Macromolecules*, **25,** 3174.
[31] Wright, P. V., 1995, *J. mater. Chem.*, **5,** 1275.
[32] Gohy, J. F., Vanhoorne, P., and Jèrôme, R., 1996, *Macromolecules*, **29,** 776.
[33] Percec, V., Johansson, G., Heck, J., Ungar, G., and Batty, S. V., 1993, *J. chem. Soc., Perkin Trans.*, **1,** 1411.
[34] Percec, V., Johansson, G., and Rodenhouse, R., 1992, *Macromolecules*, **25,** 2563.
[35] Bengs, H., Renkel, R., and Ringsdorf, H., 1991, *Makromol. Chem., rapid Commun.*, **12,** 439.
[36] Ringsdorf, H., Wüstefeld, R., Zerta, E., Ebert, M., and Wendorff, J. H., 1989, *Angew. Chem. int. Ed. Engl.*, **28,** 914.
[37] Li, X., Goh, S. H., Lai, Y. H., and Wee, A. T. S., 2000, *Polymer*, **41,** 6563.
[38] Odinokov, S. E., Mashkovsky, A. A., Glazunov, V. P., Iogansen, A. V., and Rassadin, B. V., 1976, *Spectrochim. Acta*, **32A,** 1355.
[39] Li, X., Goh, S. H., Lai, Y. H., and Cheng, S. X., 2001, *Liq. Cryst.*, **28,** 1527.
[40] Kosaka, Y., and Uryu, T., 1995, *J. polym. Sci. A: polym. Chem.*, **33,** 2221.
[41] Imrie, C. T., Karasz, F. E., and Attard, G. S., 1991, *Liq. Cryst.*, **9,** 47.